Studies of Solvate and Inclusion Complexes of Bis[6-*O*,6-*O*′-(1,2:3,4-diisopropylidene-α-D-galactopyranosyl)-thiophosphoryl] Disulfide in the Solid State by NMR and X-ray Methods

Marek J. Potrzebowski,*,† Jarosław Błaszczyk,‡ and Michał W. Wieczorek‡

Polish Academy of Sciences, Centre of Molecular and Macromolecular Studies, Sienkiewicza 112, 90-362 Łódź, Poland, and Technical University of Łódź, Stefanowskiego 4/10, 90-924 Łódź, Poland

Received November 4, 1994®

^{31}P CP/MAS spectroscopy was used to recognize different crystallographic forms of bis[6-*O*,6-*O*′-(1,2:3,4-diisopropylidene-α-D-galactopyranosyl)thiophosphoryl] disulfide. From analysis of ^{31}P chemical shift parameters, anisotropy $\Delta\delta$, and asymmetry η it was concluded that each polymorph under investigation has *anti-anti* geometry of S=P–S–S–P=S skeleton and S=P–S angles in the range 105–107°. The P=S and P–S distances for appropriate polymorphs are almost identical. ^{2}H CP/MAS showed that solvent molecules are included in the crystallographic lattice. From line shape analysis of Pake doublets the fast molecular motion of benzene-d_6 with correlation time $\tau_c < 10^{-7}$ was established. Three different crystallographic forms of disulfide **1a–c** determined by XRD belong to different crystallographic systems and space groups. The differences are connected with kind and amount of solvent used in crystallization. Crystals of **1a** are orthorhombic, $P2_12_12_1$, with a = 10.536(4) Å, b = 25.067(4) Å, c = 28.021(5) Å, V = 7401(4) Å^3, Z = 4, D_c = 1.249(2) g cm^{-3}. Refinement using 2693 observed reflections for 811 parameters gives R = 0.067. The asymmetric part of the unit cell contains one molecule of **1** with one molecule of benzene and one molecule of hexane. Crystals of **1b** are monoclinic, space group $P2_1$, with a = 10.4293(8) Å, b = 28.206(2) Å, c = 12.105(1) Å, β = 90.696(8)°, V = 3560.6(7) Å^3, Z = 2, D_c = 1.367(2) g cm^{-3}. Refinement using 6504 observed reflections for 775 parameters gives R = 0.060. The asymmetric part of the unit cell contains one molecule of **1** with two molecules of chloroform. Crystals of **1c** are trigonal, space group $P3_2$, with a = b = 11.861(1) Å, c = 44.679(3) Å, V = 5443(3) Å^3, Z = 3, D_c = 1.266(2) g cm^{-3}. Refinement using 3191 observed reflections for 811 parameters gives R = 0.040. The asymmetric part of the unit cell contains one molecule of **1** with two molecules of benzene. Variable temperature ^{31}P CP/MAS and ^{2}H CP/MAS studies revealed that crystals of **1a** and **1c** form inclusion complexes with solvent which are unstable and undergo a phase transition below the melting point.

Introduction

Phosphorylated sugars are of particular interest due to their biological functions and synthetic applications. The glycosyl phosphosugars are fragments of several glycoproteins, and yeast phosphoglycans as well are present in the cell walls and capsules of numerous bacteria as structural blocks of the poly(glycosyl phosphates).[1-4] β-D-Fructose-2,6-bisphosphate has recently been reported as an important regulator of glycolysis and gluconeogenesis.[5] Disaccharide phosphates are considered as microbiols and antitumor agents.[6] Other phosphorylated derivatives are components of the endotoxic lipopolysaccharides.[7] Further, the thio analogs of naturally occurring phosphates are potentially valuable as regulators, activators, or inhibitors of metabolism.[8]

Chart 1

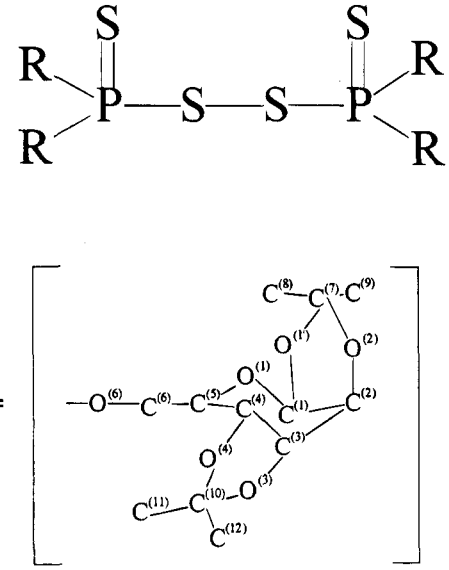

Several synthetic methods have been developed in order to synthesize phosphorylated sugars, and some of them were recently reviewed.[9] Kochetkov and co-workers have shown that the hydrogen phosphate approach commonly used for preparation of oligo- and polynucleo-

* To whom correspondence should be addressed.
† Polish Academy of Sciences.
‡ Technical University of Łódź.
® Abstract published in *Advance ACS Abstracts,* April 1, 1995.

(1) von Figura, K.; Hasalik, A. *Annu. Rev. Biochem.* **1986**, *55*, 167–190.
(2) Marchase, R. B.; Koro, L. A.; Kelly, C. M.; Mc Clay, D. R. *Cell* **1982**, *28*, 813–820.
(3) Kenne, L.; Lindberg, B. *The Polysaccharides*; Aspinall, G. O., Ed.; Academic Press: New York, 1983; Vol. 2, pp 287–363.
(4) Barreto-Bergter, E.; Gorin, P. A. J. *Adv. Carbohydr. Chem. Biochem.* **1983**, *41*, 67–103.
(5) Nicotra, F.; Panza, L.; Russo, G.; Senaldi, A.; Burlini, N.; Tortora, P. *J. Chem. Soc. Chem. Commun.* **1990**, 1396.
(6) Kennedy, J. F.; White, C. A. *Bioactive Carbohydrates*; Ellis Hortwood Ltd.: West Sussex, 1983.
(7) Unger, F. M. *Adv. Carbohydr. Chem. Biochem.* **1981**, *38*, 323.
(8) Eckstein, F. *Annu. Rev Biochem.* **1985**, *54*, 367.
(9) Vasella, A.; Baudin, G.; Panza, L. *Heteroatom. Chem.* **1991**, *1*, 151 and references cited therein.

0022-3263/95/1960-2549$09.00/0

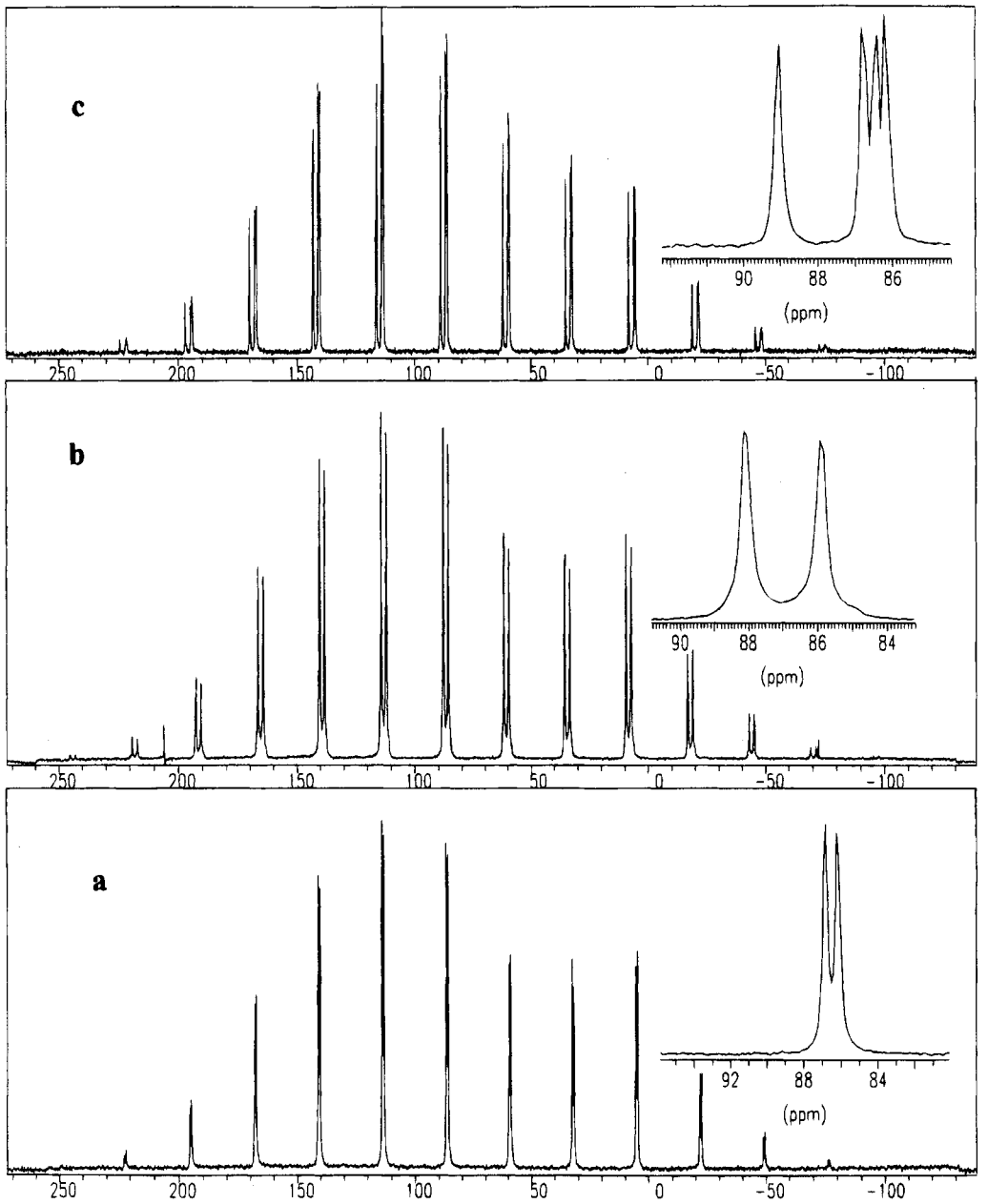

Figure 1. ^{31}P CP/MAS experimental spectra of polymorphs of bis[6-*O*,6-*O'*-(1,2:3,4-diisopropylidene-α-D-galactopyranosyl)-thiophosphoryl] disulfide (**1**). All spectra have 8K data points, a contact time of 5 ms, and 100 scans. The top traces display the expanded central part of spectra: (a) polymorph **1a**, ν_{rot} = 3384 Hz, (b) polymorph **1b**, ν_{rot} = 3187 Hz, (c) polymorph **1c**, ν_{rot} = 3302 Hz.

sides can be adopted for synthesis of linked glycosyl phosphosugars.[10] This class of compounds can also be synthesized with good yield employing the phosphate triester method as recently reported by Thiem et al.[11] The derivatives of *O*-glycosyl and *S*-glycosyl phosphorothioate are typically obtained in the substitution reaction of sugar halides or in the addition reaction to unsaturated sugars with appropriate phosphorus compounds.[12]

In this paper we report that bis[6-*O*,6-*O'*-(1,2:3,4-diisopropylidene-α-D-galactopyranosyl)thiophosphoryl] disulfide (Chart 1) synthesized in the reaction of the suitable, blocked sugar with phosphorus pentasulfide in the presence of tertiary amine shows unique properties

Table 1. ^{31}P Chemical Shift Parameters for Three Polymorphs of Bis[6-*O*,6-*O'*-(1,2:3,4-diisopropylidene-α-D-galactopyranosyl)thiophosphoryl] Disulfide (1)[a]

disulfide	δ_{iso} (ppm)	δ_{11} (ppm)	δ_{22} (ppm)	δ_{33} (ppm)	$\Delta\delta$ (ppm)	Ω (ppm)	η	κ
1a	86.8	196.6	105.0	−41.2	192	238	0.72	0.23
	86.2	197.1	102.0	−40.7	190	237	0.75	0.20
1b	88.0	200.2	103.2	−39.2	191	239	0.76	0.19
	85.9	200.4	96.2	−39.0	187	239	0.83	0.13
1c	89.1	203.5	102.8	−39.1	192	242	0.79	0.17
	86.8	189.9	104.7	−34.2	182	224	0.70	0.24
	86.5	199.7	101.8	−42.1	193	242	0.76	0.19
	86.1	196.6	103.6	−41.8	192	239	0.73	0.22

[a] Estimated errors in δ_{11}, δ_{22}, δ_{33}, and $\Delta\delta$ are ±5 ppm; errors in δ_{iso} are ±0.2 ppm. The principal components of the chemical shift tensor are defined as follows: $\delta_{11} > \delta_{22} > \delta_{33}$. The isotropic chemical shift is given by $\delta_{iso} = (\delta_{11} + \delta_{22} + \delta_{33})/3$.

(10) Nikolaev, A. V.; Ivanova, I. A.; Shibaev, V. N.; Kochetkov N. K. *Carbohydr. Res.* **1990**, *204*, 65–78.
(11) Thiem, J.; Franzkowiak, M. *J. Carbohydr. Chem.* **1989**, *8*, 1–28.
(12) Bogusiak, J.; Szeja, W. *J. Carbohydr. Chem.* **1991**, *10*, 47–54 and references cited therein.

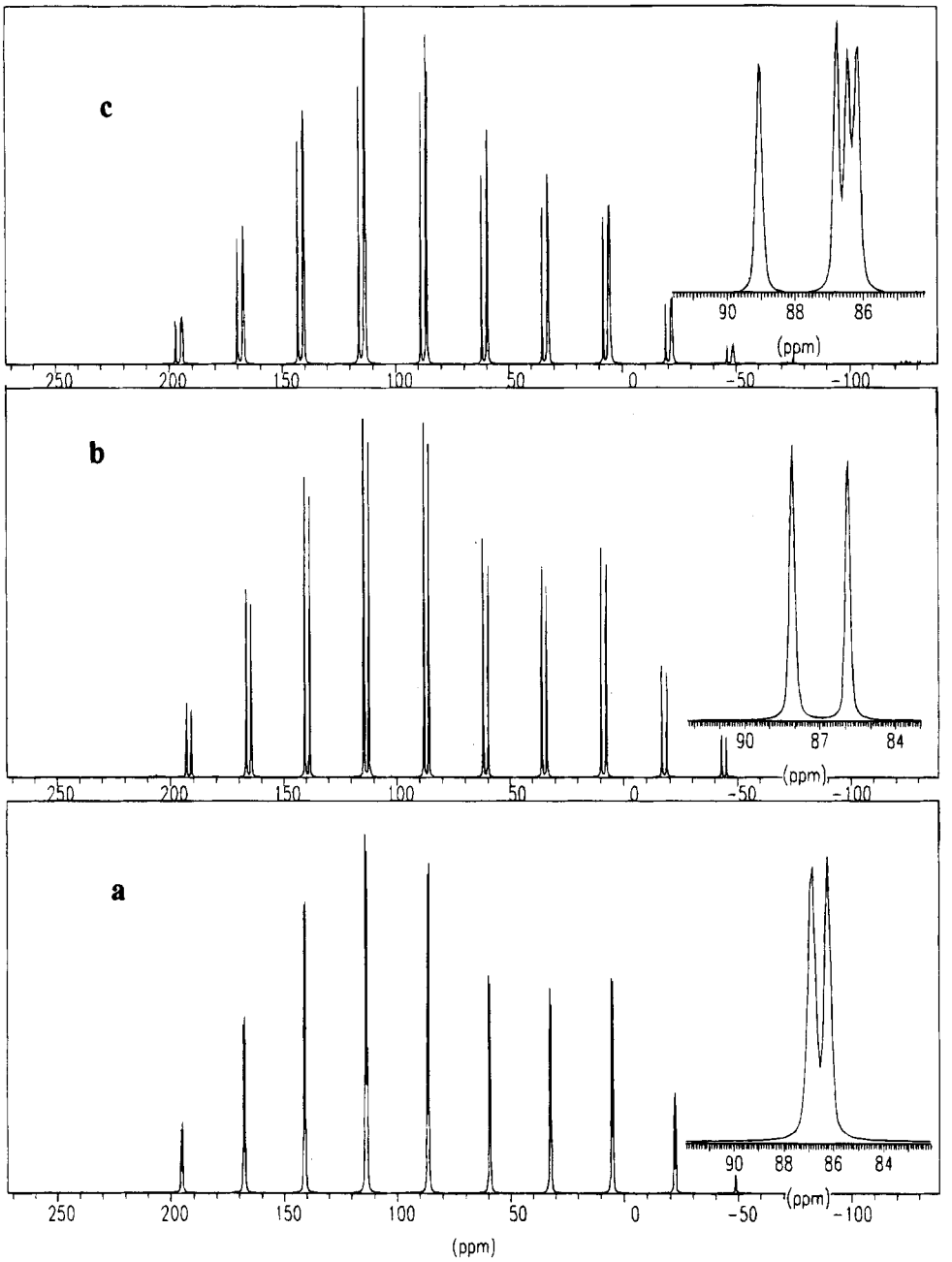

Figure 2. ^{31}P CP/MAS theoretical spectra of polymorphs of bis[6-*O*,6-*O'*-(1,2:3,4-diisopropylidene-α-D-galactopyranosyl)-thiophosphoryl] disulfide (**1**). Spectra were calculated employing the MASNMR program. The top traces display the expanded central part of the spectra: (a) polymorph **1a**, ν_{rot} = 3384 Hz, (b) polymorph **1b**, ν_{rot} = 3187 Hz, (c) polymorph **1c**, ν_{rot} = 3302 Hz.

in the solids forming different types of solvate and inclusion complexes.

The inclusion compounds and solvates have been very well known since the early studies of organic chemistry. The history and background of inclusion phenomenon have been exhaustively reviewed by Powell.[13] Owing to their significance in pure and applied chemistry, sugar derivatives play a central role in the chemistry of inclusion complexes. The different cyclodextrin analogs are used both for separation of the stereoisomers as well as models for studies of enzymatic reactions.[14,15] The organophosphorus compounds have also been found to be interesting models for studies of the inclusion phenomena. As shown by Allcock the investigation of cyclophosphazane inclusion adducts can provide invaluable information about the nature of the host–guest interaction as well as molecular motion of the guest molecule.[16]

X-ray diffraction (XRD) and ^{2}H, ^{31}P solid-state NMR data for different inclusion complexes and solvate of phosphorosugar disulfide **1** are reported. As will be shown, the combination of both techniques provides

(13) Powell, H. M. Vol. 1, Structural Aspects of Inclusion Compounds Formed by Inorganic and Organometallic Host Lattice. In Inclusion Compounds; Atwood, J. L., Davies, J. E. D., MacNicol, D. D., Eds.; Academic Press: New York, 1984; Vol. 1, Chapter 1, pp 1–28.

(14) Vögtle, F. *Bioorganic Model Compounds.* In *Supramolecular Chemistry*; John Wiley and Sons: New York, 1991; Chapter 4, pp 135–170.

(15) Tabushi, I. *Acc. Chem. Res.* **1982**, *15*, 66–72.

(16) Allcock, H. R. *Structural Aspects of Inclusion Compounds Formed by Inorganic and Organometallic Host Lattice.* In *Inclusion Compounds*; Atwood, J. L., Davies, J. E. D., MacNicol, D. D., Eds.; Academic Press: New York, 1984; Vol. 1, Chapter 8, pp 351–374.

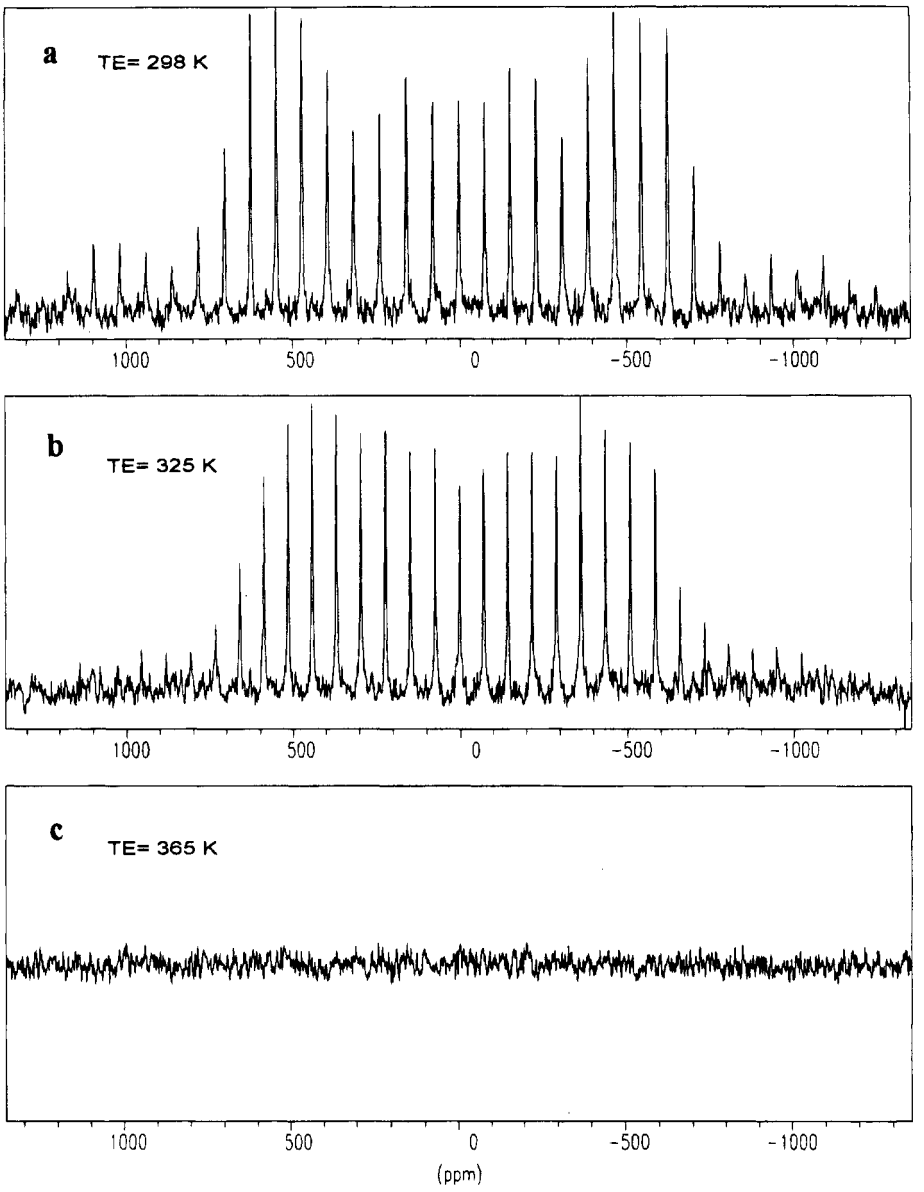

Figure 3. Variable temperature ^2H CP/MAS experimental spectra of polymorph **1c**. All spectra have 8K data points, a contact time of 7 ms, and 1000 scans (a) at 298 K, (b) at 325 K, and (c) at 365 K.

complementary information about the structure and dynamics of host/guests molecules.

Results and Discussion

^{31}P CP/MAS Solid State NMR Studies. In our recent papers it was shown that ^{31}P CP/MAS is a very powerful technique to study the structural properties of bis(organothiophosphoryl) disulfides.[17-23] From analysis of shielding parameters and ^{31}P principal components of the chemical shift tensor, δ_{ii}, conclusions regarding the geometry of the molecule may be drawn. Moreover, it was concluded that this technique is very sensitive to molecular symmetry and molecular packing.

Figure 1 displays the ^{31}P CP/MAS spectra of bis[6-*O*,6-*O'*-(1,2:3,4-diisopropylidene-α-D-galactopyranosyl)thiophosphoryl] disulfide (**1**) recorded at room temperature. In the spectra, each sample shows a number of spinning sidebands due to large chemical shielding anisotropy (CSA). The phosphorus can be considered as an isolated nucleus because adjacent atoms in the tetrahedral arrangement are zero spin nuclei. The interactions with active isotopes of sulfur, carbon, and oxygen at natural abundance are below the detectable limit and were neglected. The dipolar coupling from the protons of galactopyranoses was eliminated by proton decoupling during data acquisition.

Figure 1a-c show the spectra of the disulfides **1** crystallized under different conditions or employing

(17) Chu, P.-J.; Potrzebowski, M. J. *Magn. Reson. Chem.* **1990**, *28*, 477-485.
(18) Potrzebowski, M. J. *J. Chem. Soc., Perkin Trans. 2* **1993**, 63-66.
(19) Potrzebowski, M. J.; Reibenspies, J. H.; Zhong, Z. *Heteroatom. Chem.* **1991**, *2*, 455-460.
(20) Knopik, P.; Łuczak, L.; Potrzebowski, M. J.; Michalski, J.; Błaszczyk, J.; Wieczorek, M. W. *J. Chem. Soc., Dalton Trans.* **1993**, 2749-2757.
(21) Potrzebowski, M. J.; Grossman, G.; Błaszczyk, J.; Wieczorek, M. W.; Sieler, J.; Knopik, P.; Komber, H. *Inorg. Chem.* **1994**, *33*, 4688-4695.
(22) Potrzebowski, M. J.; Michalski, J. ^{31}P High-Resolution Solid-State NMR Studies of Thiophosphoroorganic Compounds. In *Phosphorus-31 NMR Spectra Properties in Compound Characterization and Structural Analysis*; Quin, L. D., Verkade, J. G., Eds.; VCH: New York, 1994; Chapter 31, pp 413-426.
(23) Potrzebowski, M. J. *Phosphorus, Sulfur Silicon* **1993**, *74*, 435-436.

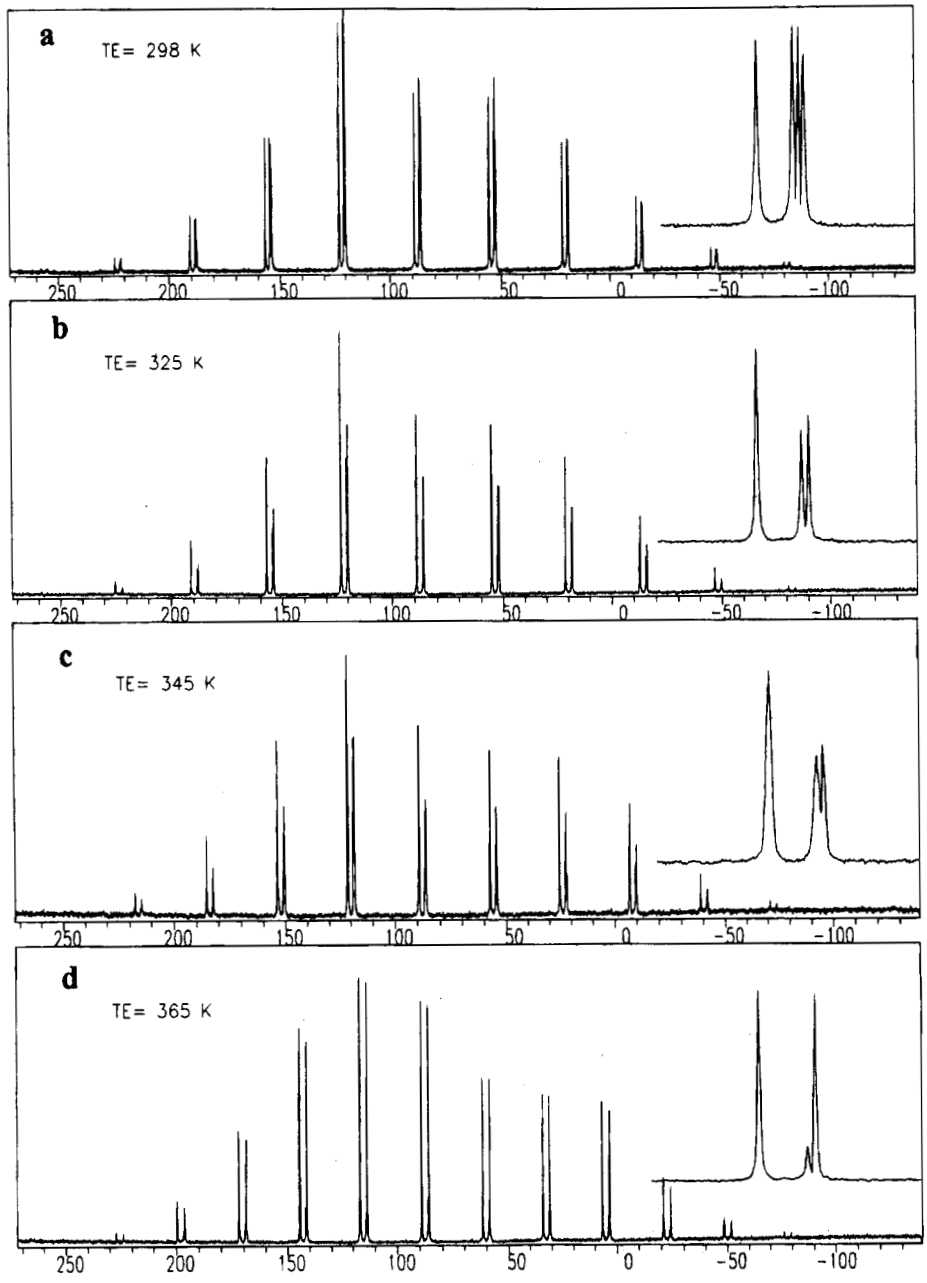

Figure 4. Variable temperature ^{31}P CP/MAS experimental spectra of polymorph **1c**. All spectra have 8K data points, a contact time of 5 ms, and 100 scans (a) at 298 K, (b) at 325 K, and (c) at 345 K and (d) at 365 K.

different solvents. From spectra analysis the differences are apparent. Figure 1a presents the disulfide **1a** crystallized from a mixture of benzene:hexane (v:v) at 268 K. The top trace displays the isotropic part of the spectrum with two clearly cut peaks found at $\delta = 86.8$ ppm and $\delta = 86.2$ ppm. By analogy with previous studies showing that ^{31}P CP/MAS can distinguish the number of crystallographically nonequivalent sites, it is concluded that each isotropic resonance represents the asymmetric part of the unit cell.[18,19] Judging from a similar CSA sideband pattern and small differences in isotropic chemical shifts, it is further concluded that the local environment of both phosphorus sites is almost identical.

Figure 1b shows the spectrum of disulfide **1b** crystallized from chloroform by slow isothermal evaporation of solvent. As in the case of **1a** the spectrum consists of two sideband systems. At first glance it is apparent that the spinning sideband intensities for crystallographic modifications **1a** and **1b** are similar. The signals for the latter are separated by 2.1 ppm (88.0 ppm and 85.9 ppm). It is speculated from NMR data for **1b** that molecular structures of both polymorphs are similar and that again each resonance represents phosphorane in a molecule within the asymmetric part of the unit cell.

The spectrum of disulfide **1c** (Figure 1c) crystallized at room temperature from benzene by slow diffusion of hexane into the mixture is found to be more complex. The expanded isotropic part of the spectrum shows four resonances which belong to two sets of sideband patterns. The appropriate signals are separated by 2.3 and 0.4 ppm. In order to study in detail the structure and properties of polymorph **1c**, results were obtained from analysis of the principal elements of ^{31}P chemical shifts tensors and shielding parameters, and these data were compared with the results for **1a** and **1b** as well as other bis(organothiophosphoryl) disulfides.[22]

The principal components of the ^{31}P chemical shift tensors δ_{ii} were calculated from spinning sideband intensities employing the MASNMR program which is

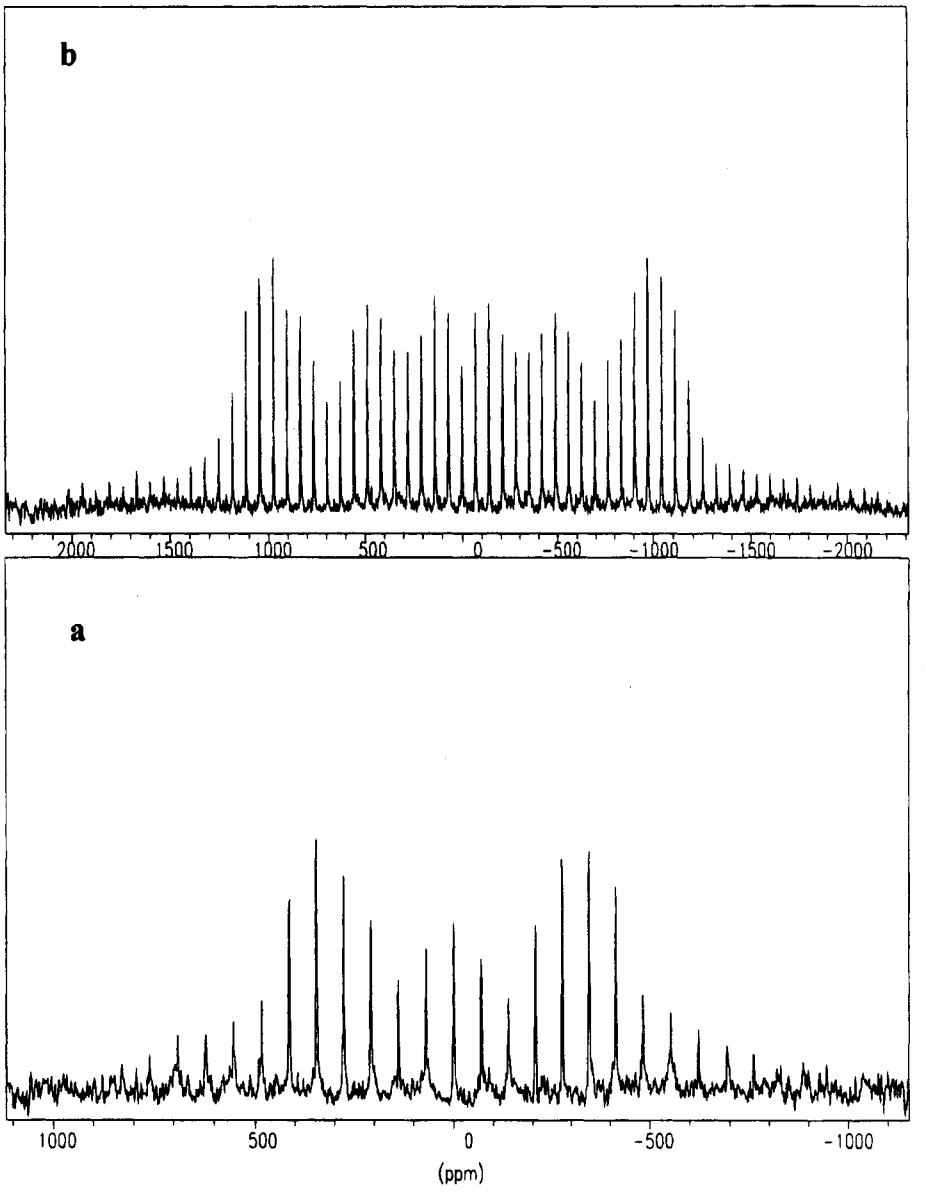

Figure 5. 2H CP/MAS experimental spectra of polymorph **1b** (b) and polymorph **1a** (a). Both spectra have 8K data points, a contact time of 7 ms, and 1000 scans.

based on the Berger–Herzfeld algorithm.[24,25] The calculated values of principal tensor elements δ_{ii} and shielding parameters are given in Table 1. The accuracy of calculations was confirmed by comparison with theoretical spectra shown in Figure 2.

The ^{31}P chemical shift parameters can be correlated with the molecular structure of S=P–S–S–P=S unit as shown elsewhere.[18,22] The linear relationship between anisotropy $\Delta\delta$, asymmetry η, and S=P–S angles was established. It was found that $\Delta\delta$ in the range 180–190 ppm and η in the range 0.70–0.80 correspond to S=P–S angles equal to 105–107°. The values obtained in this work (Table 1) show that for polymorphs **1a–c** the S=P–S angles are in this region. Moreover, the calculated values of δ_{22} and δ_{33} of principal elements of ^{31}P chemical shift tensor show that P–S and P=S distances for all polymorphs are identical. Comparing chemical shift parameters indicates that molecular structures within crystallographic unit cells of **1a–c** are similar, and it is very likely that the S=P–S–S–P=S backbone adopts a planar, *anti-anti* geometry. Consequently, the differences in number and separation of resonances are due to differences in the crystal structures. The occluded solvents have a significant influence on arrangement of disulfide molecules in the crystal lattice.

^{2}H CP/MAS NMR and ^{31}P CP/MAS NMR Variable Temperature Studies. In order to reveal the presence of solvent molecules in the crystal lattice of polymorphs **1a–c**, ^{2}H CP/MAS was performed with material crystallized from benzene-d_6 or chloroform-*d*. Poupko and coworkers have demonstrated that ^{2}H MAS spectroscopy offers better sensitivity than commonly used quadrupole-echo pulse techniques.[26] Zumbulyadis and O'Relly as well as Potrzebowski et al. have demonstrated that a further gain of sensitivity can be attained in cross-polarization step.[27,28] Lastly, all information regarding the molecular motion can be obtained from line shape analysis of high-resolution spectra, and in addition, CP/

(24) Jeschke, G.; Grossmann, G. *J. Magn. Reson.* **1993**, *A103*, 323–328.
(25) Herzfeld, J.; Berger, A. *J. Chem. Phys.* **1980**, *73*, 6021.
(26) Poupko, R.; Olender, Z.; Reichert, D.; Luz, Z. *J. Magn. Reson.* **1994**, *106*, 113.
(27) Zumbulyadis, N.; O'Reily, J. M. *J. Am. Chem. Soc.* **1993**, *115*, 4407.

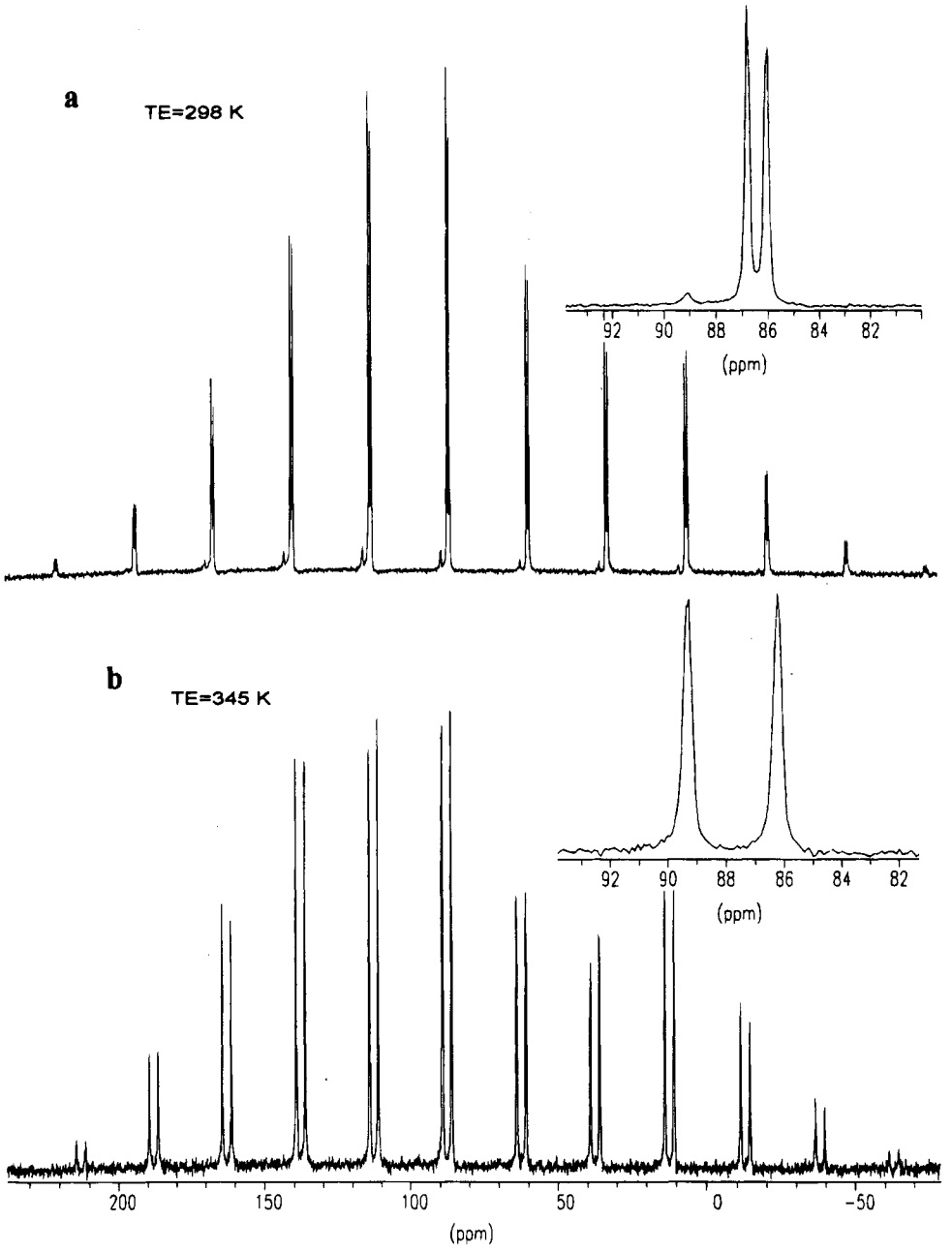

Figure 6. Variable temperature ^{31}P CP/MAS experimental spectra of polymorph **1a**. Both spectra have 8K data points, a contact time of 5 ms, and 100 scans (a) at 298 K and (b) at 345 K.

MAS methods based on cross polarization from protons to deuterium can be used to probe microscopic heterogeneity.

Figure 3 displays the ^2H CP/MAS spectrum of disulfide **1c** crystallized from benzene-d_6/hexane. The spinning sidebands form a characteristic Pake doublet pattern that can be used in the analysis of molecular motion.[29,30] As shown in Figure 3a the splitting between singularities is found to be 59 kHz for a sample recorded at 298 K. For the static C–D bond the splitting is generally 128 kHz, *i.e.*, three-fourths the quadrupole coupling constants.[31] The value 59 kHz indicates the fast molecular motion with a correlation time $\tau_c < 10^{-7}$ of occluded benzene molecules. The spectra recorded employing MAS NMR and CP/MAS NMR techniques showed the gain of signal intensity for the latter method. Because efficient cross-polarization requires close proximity of the ^1H and ^2H nuclei, this result suggests a short distance between host and guest molecules.

At 325 K, disulfide **1c** undergoes a second-order phase transition. Judging from the line shape of the ^2H CP/MAS spectrum of benzene-d_6 (Figure 3b), the molecular motion of the guest molecule in this case is more complex. First, the splitting between singularities is 33 kHz. Second, the spinning sidebands form a pattern that suggests that motional averaging of the field gradient tensor is not axially symmetric. The usual line shape with $\eta > 0$ arises when deuterated phenyl rings undergo a 180° ring flip along the 1,4-phenylene axis.[31] Thus, it can be speculated that at higher temperature the molecular motion of benzene becomes a combination of

(28) Potrzebowski, M. J.; Wasiak J.; Ciesielski, W.; Klinowski, J. *J. Magn. Reson.* Submitted for publication.
(29) Spiess, H. W. *Adv. Polym. Sci.* **1985**, *66*, 23.
(30) Kristensen, J. H.; Bildsoe, H.; Jakobsen H. J.; Nielsen N. Ch. *J. Magn. Reson.* **1992**, *92*, 443.
(31) Jelinski, L. W. In *High Resolution NMR Spectroscopy of Synthetic Polymers in Bulk*; Komoroski, R. A., Ed.; VCH Publishers: New York, 1986; Chapter 10, pp 335–364.

Table 2. Crystal Data and Experimental Details for Inclusion Complexes of Bis[6-*O*,6-*O'*-1,2:3,4-diisopropylidenegalactopyranosyl)thiophosphoryl] Disulfide (1)

	1a	1b	1c
molecular formula	$C_{48}H_{76}O_{24}P_2S_4 \times (C_6H_6)$-$(C_6H_{14})$	$C_{48}H_{76}O_{24}P_2S_4 \times 2(CHCl_3)$	$C_{48}H_{76}O_{24}P_2S_4 \times 2(C_6H_6)$
$F(000)$	1391.6	1466.1	1383.6
crystallizn solvent	benzene/hexane	chloroform	benzene
crystallographic syst	orthorhombic	monoclinic	trigonal
space grp	$P2_12_12_1$	$P2_1$	$P3_2$
a (Å)	10.536(4)	10.4293(8)	11.861(1)
b (Å)	25.067(4)	28.206(2)	11.861(1)
c (Å)	28.021(5)	12.105(1)	44.679(3)
β (deg)	(90)	90.696(8)	(90)
V (Å^3)	7401(4)	3560.6(7)	5443(3)
Z	4	2	3
D_c (g/cm^3)	1.249(2)	1.367(2)	1.266(2)
μ (cm^{-1})	2.3	43.5	21.9
cryst. dimens (mm)	0.4, 0.4, 0.5	0.2, 0.2, 0.5	0.2, 0.5, 0.5
maximum 2θ (deg)	50	150	150
radiatn, λ (Å)	Mo Kα, 0.71073	Cu Kα, 1.54178	Cu Kα, 1.54178
scan mode	$\omega/2\theta$	$\omega/2\theta$	$\omega/2\theta$
scan width (deg)	1.32 + 0.35 tan θ	0.90 + 0.14 tan θ	0.70 + 0.14 tan θ
hkl ranges	h = 0−12	h = 0−13	h = 0−14
	k = 0−29	k = 0−35	k = 0−14
	l = 0−33	l = −15−15	l = 0−56
EAC correction:			
min	0.8860	0.8311	0.9606
max	0.9983	0.9990	0.9976
avg	0.9204	0.9208	0.9841
no. of reflns:			
unique	7192	7873	4367
with $I \geq 3\sigma(I)$	2693	6504	3191
no. of param	811	775	811
weighting scheme	unit weight	unit weight	unit weight
largest peak (eÅ^{-3})	0.627	0.513	0.562
largest shift/error	0.01	0.02	0.01
R	0.067	0.060	0.040

vibrations and 180° flips. A second explanation may assume the presence of two or more benzene molecules in the crystal lattice having different mobilities. In the latter case, the line shape would be a superposition of two (or more) different Pake's doublets. It must be stressed that in order to receive detailed information about guest molecule dynamics more advanced studies should be carried out. It is noteworthy that after the sample was recorded to 298 K, this same spinning sideband pattern is observed as seen in Figure 3b. This means that changes in molecular dynamics are related to an irreversible phase transition below the melting point of crystals **1c**. At 355 K (Figure 3c) benzene diffuses out from crystal lattice.

^{2}H CP/MAS results are very consistent with ^{31}P CP/MAS variable temperature experiments. Figure 4 shows the phosphorus high-resolution spectra of disulfide **1c** recorded at different temperatures.

Analysis of the isotropic part of the ^{31}P spectra indicates that crystals of **1c** are unstable and undergo phase transition well below its melting temperature, 426−428 K. At 325 K (Figure 4b), three instead of four resonances (Figure 4a, T = 298 K) are observed; at higher temperature (Figure 4c, T = 345 K) the upfield resonances are separated only by 0.2 ppm. At 365 K (Figure 4d) the spectrum is very similar to that recorded for disulfide **1b**. Again, the phase transition is irreversible; after sample was cooled to room temperature a spectrum similar to Figure 4d was obtained. Analysis of ^{31}P chemical shift parameters unambiguously reveals that during heating the molecular structure of disulfide **1c** is not changed. The S=P−S−S−P=S backbone is rigid and does not undergo rotation around the P−S and S−S bonds over a broad range of temperatures.

Table 3. Selected Bond Distances (Å), Bond Angles (deg), and Torsion Angles (deg) in Inclusion Complexes 1a−c[a]

	1a	1b	1c
bond distances			
S1−S2	2.061(6)	2.075(3)	2.065(3)
S1−P1	2.097(6)	2.091(2)	2.090(2)
S2−P2	2.096(6)	2.086(3)	2.088(3)
S3=P1	1.901(6)	1.899(3)	1.901(4)
S4=P2	1.894(7)	1.908(3)	1.907(3)
P−O1A	1.57(2)	1.581(5)	1.570(4)
P−O1B	1.60(1)	1.592(5)	1.600(6)
P−O1C	1.603(9)	1.558(5)	1.570(6)
P−O1D	1.56(2)	1.574(5)	1.597(5)
O1A−C1A	1.44(2)	1.446(9)	1.444(9)
O1B−C1B	1.44(2)	1.46(1)	1.455(8)
O1C−C1C	1.45(2)	1.463(8)	1.490(9)
O1D−C1D	1.44(2)	1.42(1)	1.448(8)
C1A−C2A	1.50(2)	1.512(9)	1.509(9)
C1B−C2B	1.57(2)	1.53(2)	1.51(1)
C1C−C2C	1.53(2)	1.501(9)	1.530(8)
C1D−C2D	1.48(2)	1.51(2)	1.48(1)
bond angles			
S2−S1−P1	108.4(2)	109.1(2)	108.2(1)
S1−S2−P2	109.1(3)	108.4(2)	107.2(1)
S1−P1=S3	106.8(2)	105.6(1)	105.1(1)
S2−P2=S4	106.9(3)	106.3(1)	107.2(2)
S−P−O1A	108.1(4)	106.8(3)	106.5(2)
S−P−O1B	106.0(4)	108.4(2)	110.0(2)
S−P−O1C	107.3(4)	108.4(2)	107.5(3)
S−P−O1D	107.1(4)	107.1(3)	108.5(2)
S=P−O1A	119.3(5)	117.9(2)	119.7(2)
S=P−O1B	117.5(5)	119.8(2)	117.7(3)
S=P−O1C	116.7(4)	118.2(2)	119.0(2)
S=P−O1D	120.1(5)	121.1(2)	118.9(2)
O1−P−O1	98.3(5)	95.7(2)	96.3(3)
	97.9(5)	96.7(2)	95.9(2)
P−O1A−C1A	121.4(9)	117.8(4)	119.9(3)
P−O1B−C1B	118.3(8)	118.9(4)	120.0(5)
P−O1C−C1C	116.6(8)	117.3(4)	117.5(4)
P−O1D−C1D	122.2(9)	119.0(4)	120.2(5)
O1A−C1A−C2A	108(1)	105.8(5)	108.4(5)
O1B−C1B−C2B	104(2)	104.0(6)	104.7(6)
O1C−C1C−C2C	106(2)	105.9(5)	102.3(4)
O1D−C1D−C2D	108(1)	108.2(6)	107.4(5)
torsion angles			
P1−S1−S2−P2	−82.2(3)	81.6(1)	−76.0(1)
S2−S1−P1−S3	−157.4(3)	158.9(1)	−161.2(1)
S1−S2−P2−S4	−160.0(3)	156.8(1)	−153.3(1)
S−S−P−O1A	−28.0(5)	−76.6(2)	−24.2(2)
S−S−P−O1B	76.6(5)	29.4(2)	71.2(2)
S−S−P−O1C	74.2(5)	−73.5(2)	77.7(2)
S−S−P−O1D	−30.0(5)	26.2(2)	−33.0(2)
S−P−O1A−C1A	−74(1)	−72.0(5)	−72.9(5)
S−P−O1B−C1B	70(1)	71.5(5)	76.6(5)
S−P−O1C−C1C	71(1)	−73.5(5)	70.2(5)
S−P−O1D−C1D	−73(1)	69.9(5)	−68.4(5)
S=P2−O1A−C1A	48(1)	47.3(5)	48.7(5)
S=P1−O1B−C1B	−49(1)	−49.8(5)	−43.7(6)
S=P2−O1C−C1C	−48(1)	46.6(5)	−51.7(5)
S=P1−O1D−C1D	48(1)	−51.9(5)	51.5(6)
O1−P−O1A−C1A	175(1)	177.8(5)	176.9(5)
O1−P−O1B−C1B	−178(1)	−176.9(5)	−171.1(5)
O1−P−O1C−C1C	−178(1)	174.9(5)	179.5(5)
O1−P−O1D−C1D	175(1)	179.8(5)	178.0(5)
P2−O1A−C1A−C2A	−167(1)	−180.0(5)	−132.7(5)
P1−O1B−C1B−C2B	−177.9(8)	160.9(4)	178.5(5)
P2−O1C−C1C−C2C	−173(2)	176.9(4)	177.3(4)
P1−O1D−C1D−C2D	−159(1)	154.8(5)	−153.9(5)

[a] Atom numbering scheme is given in Figures 7 (**1c**), 9 (**1a**), and 11 (**1b**).

Figure 5a shows the ^2H CP/MAS NMR spectrum of chloroform-*d* occluded within the crystal lattice of disulfide **1b**. The splitting between singularities taken from the Pake doublet is found to be 99 kHz. This value suggests only small amplitude motion for the guest molecules. The differences in mobilities of benzene and chloroform are presumably due to the different dipole moment (polarity) of both molecules. Variable temperature ^{31}P CP/MAS experiments revealed that **1b** is stable and does not undergo phase transition below its melting point. At 355 K chloroform molecules diffuse out from crystal lattice.

In contrast, a phase transition was monitored for polymorph **1a**. ^{31}P CP/MAS spectra (Figure 6) recorded at 345 K show that a phase change is apparent.

The spinning sideband patterns for both crystalline phases are very similar, although in this instance larger differences in isotropic chemical shifts, 2.5 ppm, are seen (Figure 6b). The difference in ^{31}P shielding of the two crystalline forms is small in this case to suggest that the molecular structure is not modified. Note that occluded benzene-d_6 has a different mobility compared to that observed for polymorph **1c**. The splitting between singularities 35 kHz obtained from line shape analysis of the spectrum shown in Figure 5b is characteristic of molecules under fast regime exchange.

XRD Studies. Crystallographic data and experimental details for disulfides **1** are shown in Table 2. Atomic coordinates and tables of bond lengths, bond angles, and torsional angles have been deposited with the Cambridge Crystallographic Data Centre. The coordinates can be obtained, on request, from the Director, Cambridge Crystallographic Data Centre, 12 Union Road, Cambridge, CB2 1EZ, UK. Selected geometrical parameters for S=P–S–S–P=S units are presented in Table 3. The ORTEP thermal ellipsoidal plot with atom numbering scheme of disulfide **1c** is shown in Figure 7. The molecular packing is shown in Figure 8.

Judging from the thermal factors of benzene, the solvent molecules are in a fast motional regime; a similar conclusion was drawn from ^2H CP/MAS experiments. Bis-[6-*O*,6-*O'*-(1,2:3,4-diisopropylidene-α-D-galactopyranosyl)-thiophosphoryl] groups are bridged by a disulfide unit. The S=P–S–S–P=S backbone adopts an *anti-anti* geometry (S=P–S–S equal to 161.2° and 153.3°) as in the case of other bis(alkoxy(thiophosphoryl) disulfides published elsewhere.[22] The thionophosphoryl (P=S) and thiolophosphoryl (P–S) bond lengths are found to be 1.901 Å, 1.907 Å, 2.090 Å, and 2.088 Å and are in the range typical for bis(organothiophosphoryl) disulfides. The same conclusion can be drawn for S=P–S angles (105.1° and 107.2°). The S–S linkage is found to be 2.065(3) Å. As shown in our previous paper the S–S bond length depends on the P–S–S–P torsional angle and reaches a minimum close to 90°.[20]

Figure 9 displays the ORTEP plot and numbering system of **1a**.

The molecular structure of **1a** is very similar to that found for **1c**. The appropriate bond lengths, bond angles, and molecular arrangement of the S=P–S–S–P=S backbone are identical (see Table 3). The significant differences are seen in the crystal structure. The crystals of **1a** are orthorhombic. Figure 10 shows the molecular packing.

Figure 11 displays the ORTEP plot of disulfide **1b** crystallized from chloroform. As in previous cases the

Table 4. Asymmetry Parameters of a Six-Membered Ring in Inclusion Complexes 1a–c

	1a				1b				1c			
	A	B	C	D	A	B	C	D	A	B	C	D
torsion angles (deg)												
C3–C2–O2–C6	73.2(15)	73.5(15)	74.6(15)	72.9(18)	–68.3(7)	–66.7(7)	–67.6(7)	–68.2(7)	70.9(8)	69.8(8)	69.6(8)	68.5(8)
C2–O2–C6–C5	–39.8(17)	–36.3(16)	–38.1(15)	–40.8(20)	33.6(8)	33.4(8)	35.4(8)	32.7(8)	–36.6(10)	–33.0(9)	–32.4(9)	–34.2(10)
O2–C6–C5–C4	–16.2(19)	–20.0(18)	–19.7(17)	–13.7(22)	21.5(9)	17.1(10)	19.2(9)	21.6(9)	–19.4(10)	–21.8(10)	–22.6(10)	–21.9(12)
C6–C5–C4–C3	37.5(20)	39.8(19)	39.8(19)	37.0(21)	–43.0(8)	–34.9(10)	–41.8(9)	–40.2(9)	41.4(10)	41.3(10)	41.3(10)	44.1(10)
C5–C4–C3–C2	–5.9(19)	–6.2(18)	–4.8(19)	–8.3(21)	10.4(8)	3.2(10)	10.8(8)	6.6(9)	–10.3(9)	–7.1(10)	–6.4(10)	–12.8(9)
C4–C3–C2–O2	–45.4(15)	–47.7(16)	–47.6(16)	–44.7(18)	42.3(7)	45.1(8)	41.2(7)	44.6(8)	–44.2(7)	–46.3(8)	–47.4(9)	–41.6(8)
asymmetry parameters												
ΔC_s^{C2}	33(2)	31(2)	31(2)	35(2)	32(1)	27(1)	33(1)	29(1)	33(1)	29(1)	28(1)	34(1)
ΔC_2^{C2-O2}	8(2)	13(2)	12(2)	5(2)	10(1)	13(1)	7(1)	14(1)	8(1)	14(1)	16(1)	8(1)

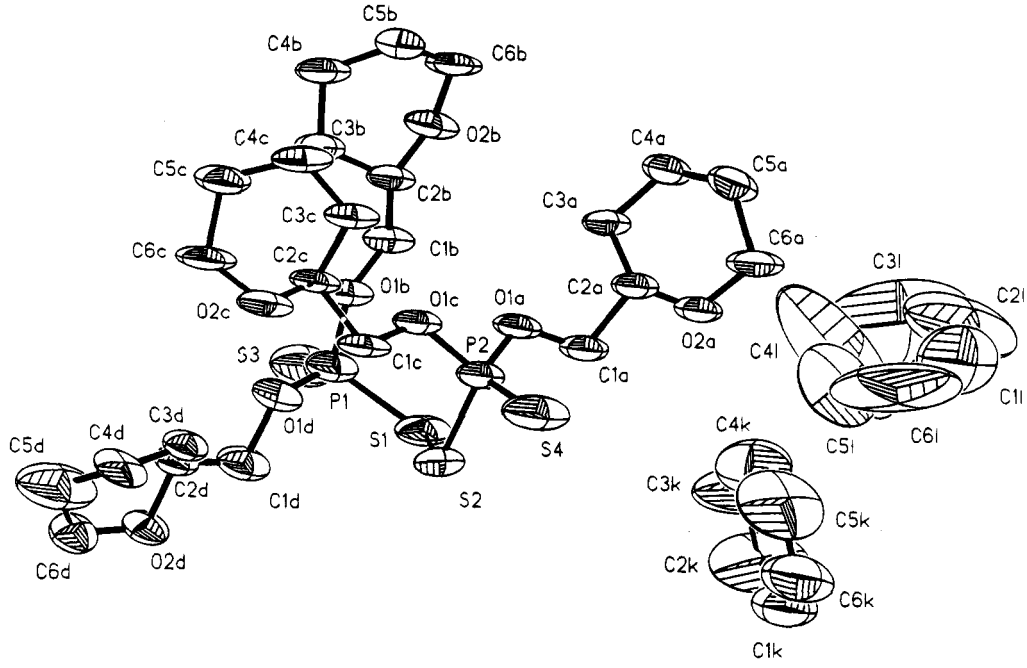

Figure 7. Thermal ellipsoidal view and atom numbering scheme of the asymmetric part of the unit cell of **1c**. The isopropylidene blocks and hydrogen atoms are not shown.

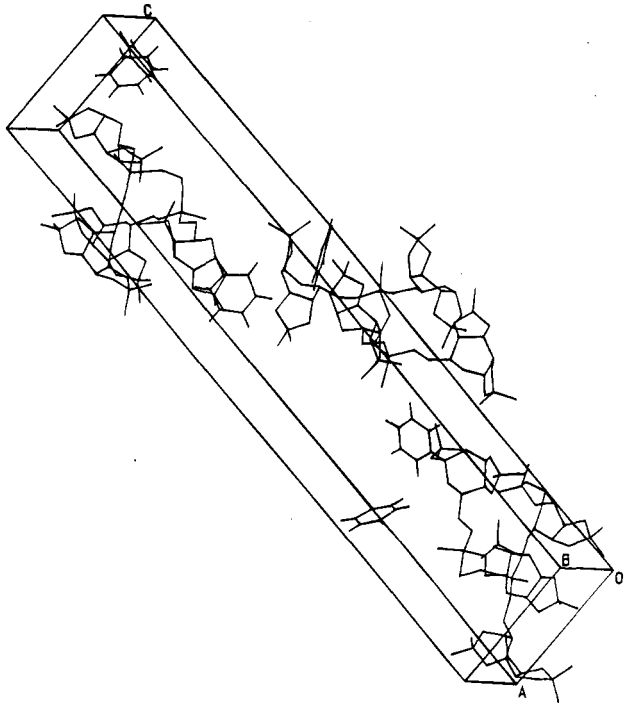

Figure 8. Unit cell of polymorph **1c** ($Z = 3$).

bis[6-*O*,6-*O'*-(1,2:3,4-diisopropylidene-α-D-galactopyranosyl)thiophosphoryl] disulfide **1b** contains a planar zigzag array of linkages, the S–S–P=S units having an *anti-anti* geometry. The resemblance of geometric parameters, bond lengths, bond angles, and torsional angles is apparent by comparison of the data given in Table 3. The molecular packing is shown in Figure 12.

Figure 13 presents the intermolecular bonding systems occuring between host and guest molecules in the crystal lattice of **1b**. The important hydrogen bonds between molecules **1** and chloroform are as follows: C1–H11···O6D with distance 2.388 Å and angle C1–H11···O6D equal to 144.3°, C1–H11···O2D with distance 2.487 Å and angle C1–H11···O6D equal to 157.9°, C1′–H11′···O6B with distance 2.196 Å and angle C1′–H11′···O6B equal to 157.2° (symmetry $1 - x$, $y - 0.5$, $1 - z$), C1′–H11′···O2B with distance 2.796 Å and angle C1′–H11′···O2B equal to 144.9° (symmetry $1 - x$, $y - 0.5$, $1 - z$). Other nonbonding contacts for distances below 3.7 Å in pictorial form are shown in Figure 13. The C–H···O hydrogen bonding between chloroform and host molecules suggests the solvate structure of **1b** crystallographic modification. This conclusion is confirmed by examination of molecular packing that consists of three unit cells (shown in the supplementary material).

In contrast, benzene molecules occluded within the crystal lattice of disulfide **1c** are trapped in cages formed by host molecules in manner typical for inclusion complexes (Figure 14b). Benzene and hexane occluded within the crystal lattice of **1a** are located in the cage and channel, respectively, formed by bis[6-*O*,6-*O'*-(1,2:3,4-diisopropylidene-α-D-galactopyranosyl)thiophosphoryl] disulfide (Figure 14a).

For disulfides **1a–c**, galactopyranose rings bonded to phosphorus are in distorted twist conformations owing to the presence of five-membered rings of the isopropylidene groups. The torsional angles and asymmetry parameters ΔC of six-membered rings[32] which describe the differences in twist conformations of rings are given in Table 4.

Summary

By means of the multitechnique approach, high-resolution solid state NMR, and X-ray diffraction, the crystal and molecular structures of different polymorphs of bis[6-*O*,6-*O'*-(1,2:3,4-diisopropylidene-α-D-galactopyranosyl)thiophosphoryl] disulfide were determined. The ^{31}P CP/MAS experiment has allowed the identification and recognition of crystallographic forms. Preliminary results regarding the geometry of the S=P–S–S–P=S backbone were obtained from ^{31}P chemical shift param-

(32) Altona, C.; Geise, H. J.; Romers, C. *Tetrahedron* **1968**, *24*, 13.

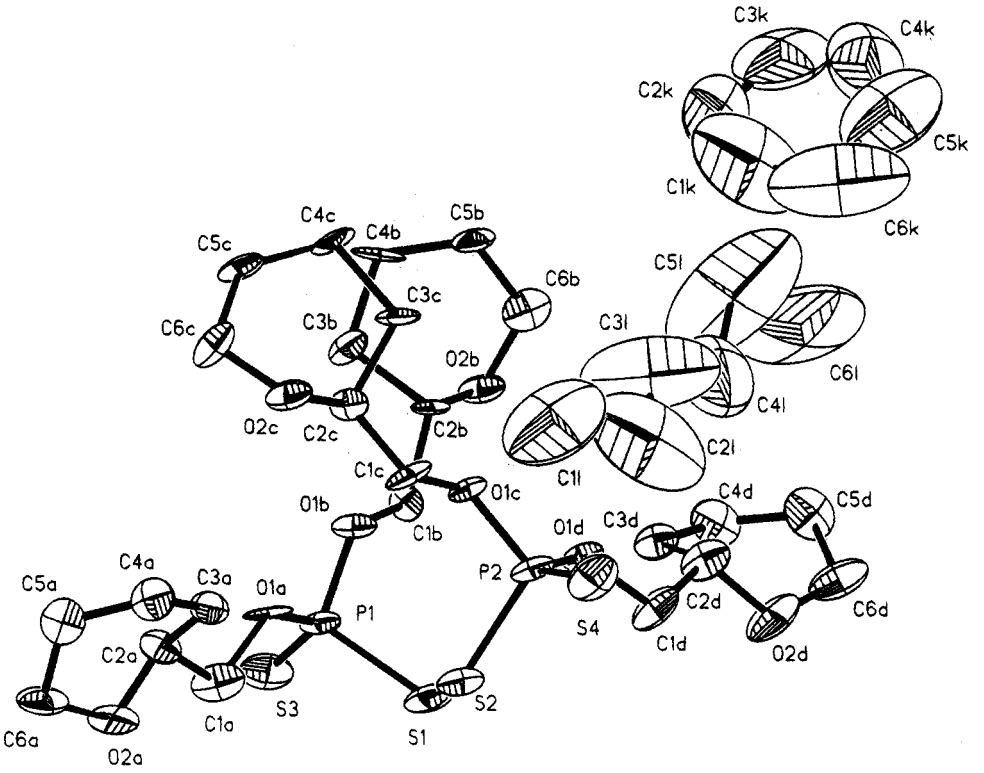

Figure 9. Thermal ellipsoidal view and atom numbering scheme of the asymmetric part of the unit cell of **1a**. The isopropylidene blocks and hydrogen atoms are not shown.

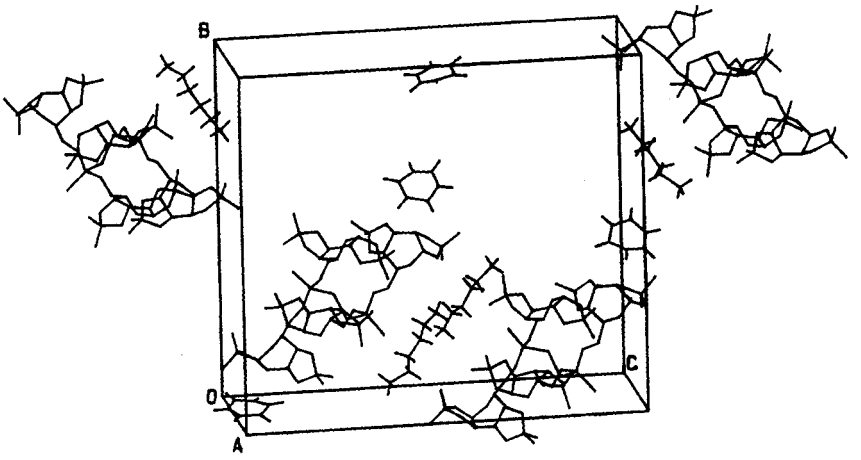

Figure 10. Unit cell of polymorph **1a** ($Z = 4$).

eters, anisotropy $\Delta\delta$, and asymmetry η. It was concluded that the S=P–S–S–P=S unit adopts the *anti-anti* geometry and S=P–S angles are in the range 105–107°.

^{2}H CP/MAS spectroscopy was used to confirm the presence of the deuterated solvents in the crystal lattice. Line shape analysis of high-resolution ^{2}H NMR spectra has revealed that benzene-d_6 molecules occluded in polymorphs **1a** and **1c** are in the fast motional regime limit with correlation time $\tau_c < 10^{-7}$. The small differences observed in mobility of guest molecules are related to the different crystal structures of **1a** and **1c**. Chloroform-*d* occluded within polymorph **1b** appears to be less mobile when compared to benzene because of its high polarity and tendency to form hydrogen bonds.

Variable-temperature NMR experiments showed that polymorphs **1a** and **1c** are unstable at higher temperatures and undergo a phase transition below the melting point. With an increase of temperature diffusion of solvent molecules from the crystal lattice was observed. Analysis of principal components of ^{31}P CSA tensors, δ_{ii}, shielding parameters, $\Delta\delta$, and η unambiguously revealed that only crystal structures are changed. Molecular structures of the complexes are not associated with the phase transition. The change of crystal structure versus the temperature was not observed for polymorph **1b**.

XRD studies of single crystals are in excellent agreement with high-resolution solid state NMR results of powdered samples. It was found that polymorphs **1a–c** have different crystal structures; **1a** is orthorhombic, space group $P2_12_12_1$, **1b** is monoclinic, space group $P2_1$, and **1c** is trigonal, space group $P3_2$. Each polymorph contains two molecules of solvent in the asymmetric part of the the unit cell: **1a**, one benzene and one hexane molecule; **1b**, two molecules of chloroform; **1c**, two molecules of benzene. The geometrical parameters for

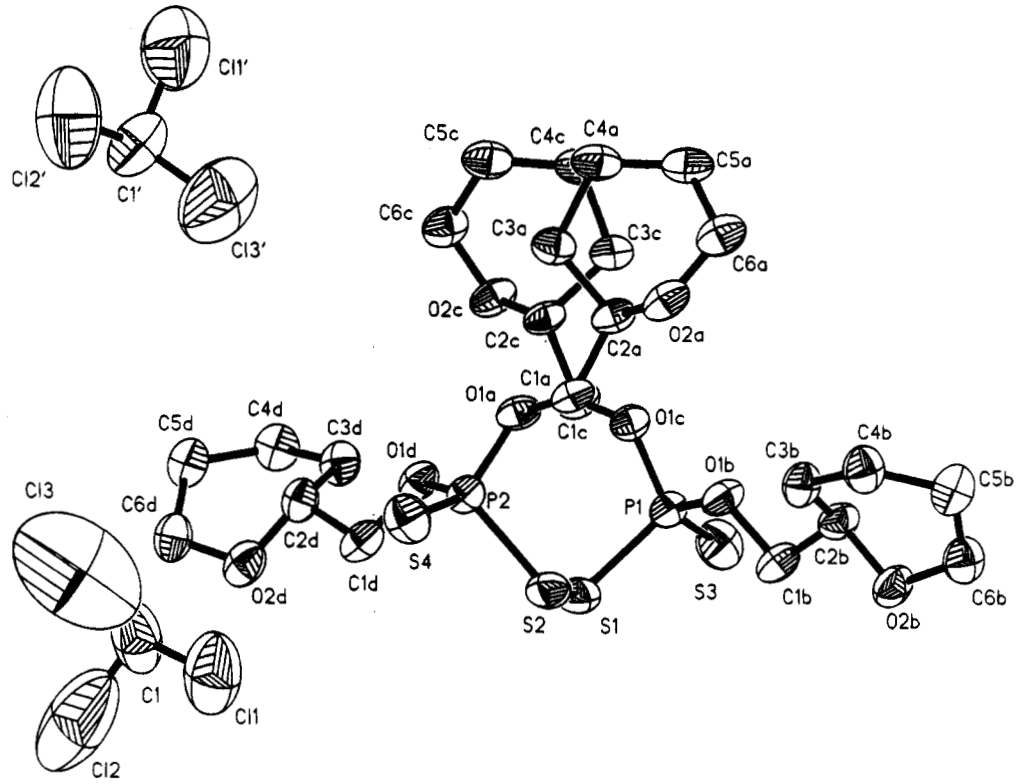

Figure 11. Thermal ellipsoidal view and atom numbering scheme of the asymmetric part of the unit cell of **1b**. The isopropylidene blocks and hydrogen atoms are not shown.

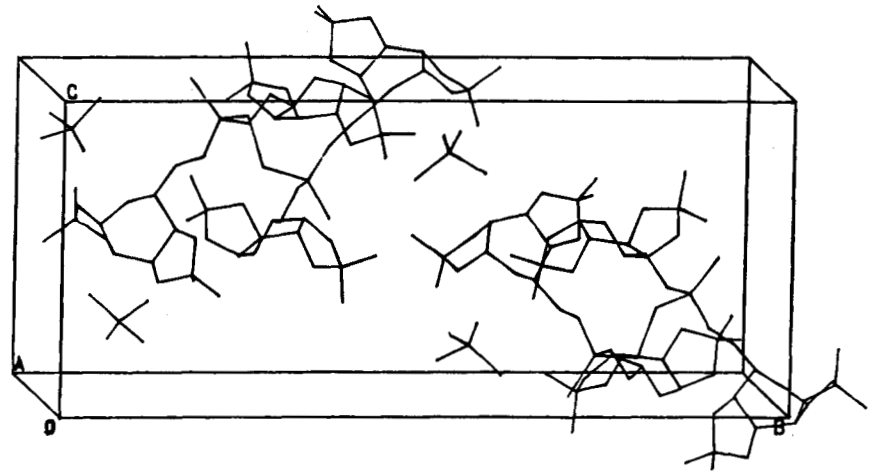

Figure 12. Unit cell of polymorph **1b** ($Z = 4$).

the S=P–S–S–P=S skeleton taken from XRD are consistent with those predicted from ^{31}P CP/MAS data.

This work shows that solid state NMR spectroscopy is a powerful method to study molecular properties of solvates and inclusion complexes. Combined with X-ray methods, NMR can provide detailed information about host/guest interactions, and, in general, contribute to our understanding the phenomenon of polymorphism.

Experimental Section

Synthesis. A 2.6 g (100 mmol) sample of 1,2:3,4-diisopropylidene-α-D-galactopyranose and 0.555 g (25 mmol) of phosphorus pentasulfide were suspended in 100 mL of dry toluene in a three-necked flask equipped with a condenser and stirrer. A 0.505 g (50 mmol) portion of triethylamine was carefully dropped at room temperature, and then the temperature was raised gradually. The mixture was refluxed for ca. 5 h up to the moment when almost all of the phosphorus pentasulfide disappeared. The hydrogen sulfide was utilized by saturated solution of sodium sulfate. The unreacted phosphorus pentasulfide was filtered off. The triethylamine 6-*O*,6-*O'*-(1,2:3,4-diisopropylidene-α-D-galactopyranosyl)thiophosphoric acid salt was acidified and extracted several times with chloroform. Thiophosphoric acid was oxidized with iodine in a mixture chloroform/water. The obtained disulfide was dried overnight in chloroform over magnesium sulfate. The solvent was removed under vacuum. A crude oil was crystallized from the mixture of benzene/hexane. Yield 60%. The molecular weight established employing FAB technique (Finnigan MAT 95 mass spectrometer) was found to be 1226 D.

X-ray Measurements. Crystal and molecular structure of three crystal forms of **1a–c** were determined by using of data collected on a CAD4 diffractometer with graphite monochromatized radiation. The observed reflections with $I \geq 3\sigma(I)$ were used to solve the structures by direct methods (SHELXS

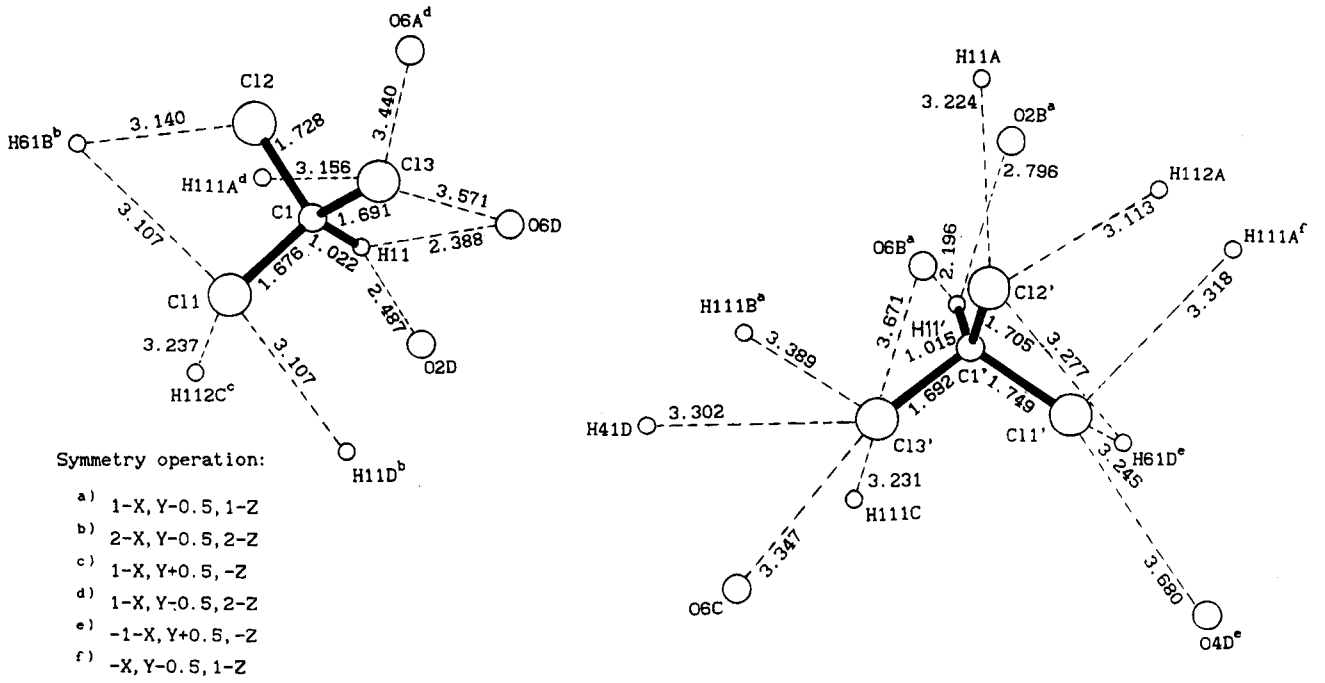

Figure 13. Environment of the chloroform molecules in the crystal lattice of **1b**. Contacts are not greater than 3.70 Å.

program[33]) and to refine them by full matrix least-squares using F's[34] (SDP computing[35]). H atoms in structures **1a**, **1b**, and **1c** were placed geometrically at idealized positions with fixed isotropic thermal parameters and not refined. Anisotropic thermal parameters were applied for all non-hydrogen atoms in all structures.

Compound **1a** crystallizes in the orthorhombic system space group $P2_12_12_1$. The unit cell parameters and other crystal data are given in Table 2. Lattice constants were refined by a least-squares fit of 25 reflections in the Θ range 8.5−12.6°. Decline in intensities of three standard reflections (3, 10, −8; 2, 6, 14; 1, 8, −7) was 8.0% during 111.0 h of exposure. Absorption correction was applied (EAC program[35]). As only a limited amount of input data is necessary for refinement of structure of **1a**, in this case the disulfide bridge with one "sugar" moiety (A, B, C, or D) has been included for calculations of anisotropical refinement, with fixing of the other parameters. The anisotropical refinement of two solvent molecules showed their very large thermal vibration in the crystal lattice.

Compound **1b** crystallizes from chloroform in monoclinic system space group $P2_1$ (Table 2). Lattice constants were refined by a least-squares fit of 25 reflections in the Θ range 21.9−26.9°. The decline in intensities of three standard reflections (2, 7, −5; 3, −7, 4; 1, −1, −6) was 51.6% during 118.2 h of exposure, so experimental data were corrected by the DECAY program[35] with correction coefficients: min = 1.000 12, max = 1.436 96 and average = 1.178 50. The absorption correction was applied (see Table 2).

Compound **1c** crystallizes in trigonal system space group $P3_2$ (Table 2). Lattice constants were refined by a least-squares fit of 25 reflections in the Θ range 23.3−24.7°. Decline in intensities of three standard reflections (3, −5, 13; 4, −6, 7; 4, −6, −5) was 7.1% during 60.1 h of exposure. The absorption correction was applied (Table 2).

NMR Measurements. Cross-polarization/magic angle spinning (CP/MAS) ^{2}H and ^{31}P NMR spectra were recorded on a Bruker MSL 300 instrument at 46.073 MHz for ^{2}H and 121.49 MHz for ^{31}P in the presence of high-power proton decoupling. Powder samples of disulfides **1** were placed in a cylindrical rotor and spun at 2.0−4.5 kHz. For the ^{2}H experiments, the field strength for ^{1}H decoupling was 1.05 mT, a contact time of 7 ms, a repetition of 6 s, and spectral width of 250 kHz were used, and 8 K data points represented the FID. Spectra were accumulated 1000 times which gave a reasonable signal-to-noise ratio.

For the ^{31}P experiments, the field strength for ^{1}H decoupling was 1.05 mT, a contact time of 5 ms, a repetition of 6 s, and spectral width of 50 kHz were used, and 8 K data points represented the FID. Spectra were accumulated 100 times which gave a reasonable signal-to-noise ratio. ^{31}P chemical shifts were calibrated indirectly through bis(dineopentoxy-(thiophosphoryl)) disulfide set at 84.0 ppm.

The principal elements of the ^{31}P chemical shift tensor and shielding parameters were calculated employing MASNMR program. The details describing the method and accuracy of calculations are exhaustively discussed elsewhere.[24,25]

The principal components δ_{ii} were used for calculation of the shielding parameters: anisotropy $\Delta\delta$, asymmetry η, span Ω, and skew κ.[36] If $|\delta_{11} - \delta_{iso}| > |\delta_{33} - \delta_{iso}|$ and $\delta_{11} > \delta_{22} > \delta_{33}$ then

$$\Delta\delta = \delta_{11} - (\delta_{22} + \delta_{33})/2 \quad (1)$$

$$\eta = (\delta_{22} - \delta_{33})/(\delta_{11} - \delta_{iso}) \quad (2)$$

If $|\delta_{11} - \delta_{iso}| < |\delta_{33} - \delta_{iso}|$ and $\delta_{11} > \delta_{22} > \delta_{33}$ then

$$\Delta\delta = \delta_{33} - (\delta_{11} + \delta_{22})/2 \quad (3)$$

$$\eta = (\delta_{22} - \delta_{11})/(\delta_{33} - \delta_{iso}) \quad (4)$$

Moreover

$$\Omega = \delta_{11} - \delta_{33} \quad (5)$$

$$\kappa = 3(\delta_{22} - \delta_{iso})/\Omega \quad (6)$$

(33) SHELXTL PC, Release 4.1. Siemens Analytical X-ray Instruments, Inc., Madison, WI 53719, 1990.
(34) *International Tables for X-ray Crystallography*; The Kynoch Press: Birmingham, England, 1974.
(35) Frenz, B. A. *SDP—Structure Determination Package*; Enraf-Nonius: Delft, Holland, 1984.
(36) Mason, J. *Solid State Nucl. Magn. Reson.* **1993**, *2*, 285−288.

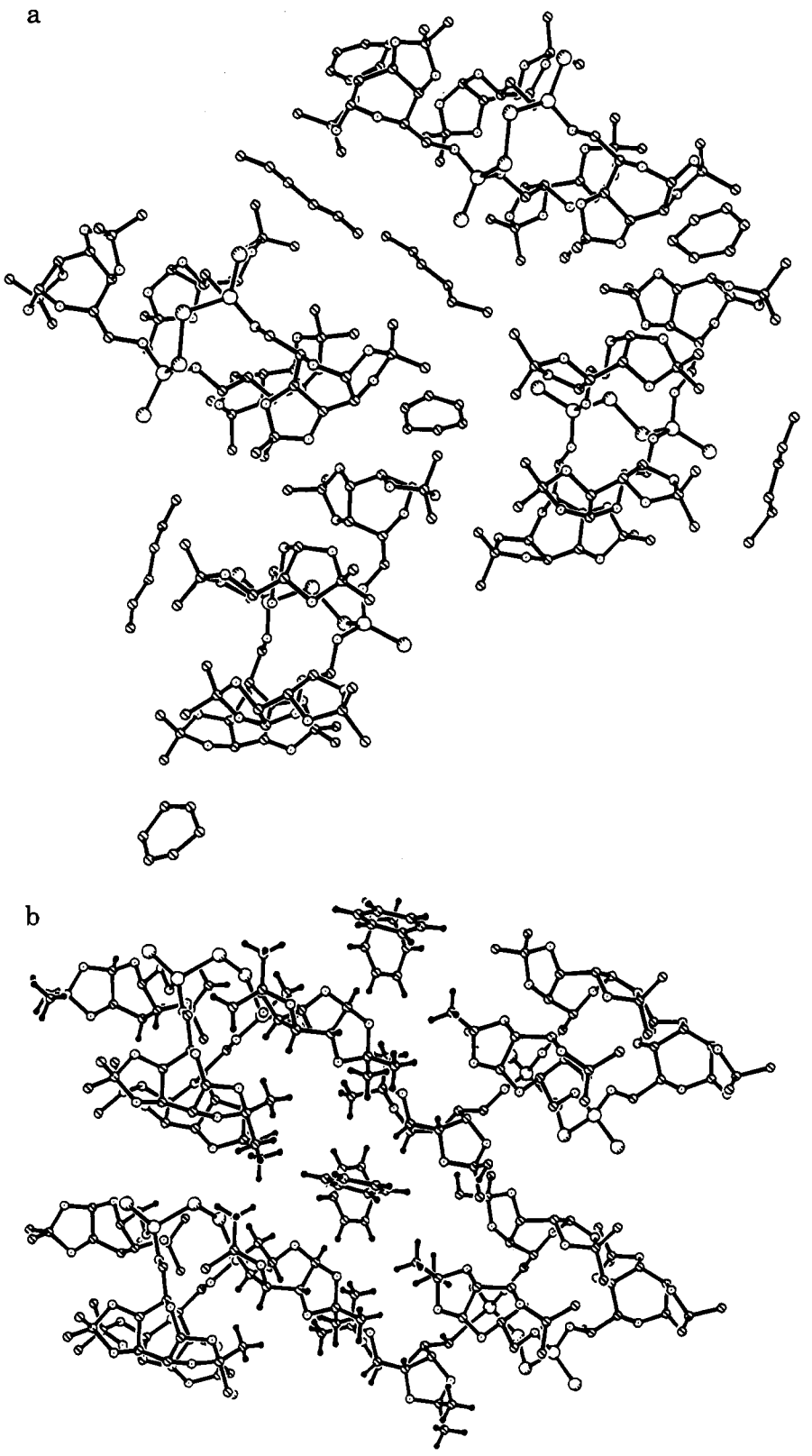

Figure 14. Molecular packing of (a) crystallographic modification of **1a** and (b) crystallographic modification of **1c**.

Acknowledgment. The authors are grateful to Prof. Jan Michalski for his interest in this project and to Mr. P. Knopik for help in the synthesis of bis-[6-*O*,6-*O*′-(1,2:3,4-diisopropylidene-α-D-galacto-pyranosyl)thiophosphoryl] disulfide. The synthetic and NMR part of this project was supported by Polish State Commitee for Scientific Research (Grant No. 2P 30303 705).

Supplementary Material Available: Molecular packing of three unit cells of **1b** (1 page). This material is contained in libraries on microfiche, immediately follows this article in the microfilm version of the journal, and can be ordered from the ACS; see any current masthead page for ordering information.

JO941853A